Accounting for multiple scattering, signal attenuation and laser extinction using Structured Laser Illumination Planar Imaging

E. Berrocal, R. Wellander and E. Kristensson
Division of Combustion Physics, Lund Institute of Technology, 22100 Lund, Sweden

Abstract

In planar laser imaging of optically dense sprays, artifacts from laser extinction and signal attenuation can only be removed if effects introduced by multiple scattering are suppressed beforehand. In this article *Structured Laser Illumination Planar Imaging* (*SLIPI*) is used to simultaneously account for multiple light scattering, monitor the incident laser power and estimate the true light transmission. By applying this novel approach and recording data at successive depths within an atomizing spray, light losses due to laser extinction and signal attenuation could be compensated for by post-processing calculations based on the Beer-Lambert law. Finally an estimation of the local extinction coefficient is extracted within the three dimensions of an inhomogeneous cloud of droplets. In this investigation an aerated water spray running at 3 bar water and 4.2 bar air injection pressure is used. Due to the internally air-assisted design of the nozzle, an optically dense cloud of fine droplets was generated with a minimum of $\sim$5 $\%$ light transmission at 2.3 cm below the nozzle tip. It is believed that this new method, which account for laser extinction and signal attenuation after the initial correction of multiple scattering by means of *SLIPI*, is key to extract and reconstruct a correct representation of the extinction coefficient within an inhomogeneous cloud of polydisperse droplets. Such quantitative information is of fundamental importance for advanced analysis, optimization and control of modern atomizing sprays.

Introduction

In spite of its whole-field detection, sharp depth of field and simplicity, laser sheet imaging of spray suffers from a number of limitations when the single scattering approximation is no longer valid and when the intermediate single-to-multiple scattering regime applies. This is problematic since the intermediate regime, characterized by a light transmission ranging from 0.0045 $\% < I_f/I_i < 36\%$, occurs in most atomizing sprays systems. The first limitation corresponds to the exponential attenuation of laser intensity as photons travel through the spray, due to scattering and absorption along the incident direction. This well known phenomenon called *laser extinction* is described by the Beer-Lambert law. Secondly, the induced signal, regardless of the scattering process involved - elastic or inelastic - is reduced between the laser sheet and the camera also according to the Beer-Lambert relation. This process is referred to as *signal attenuation* or *signal trapping*. Finally, depending on the optical thickness of the spray, photons can experience several scattering events within the sample prior to detection, a process known as *multiple scattering*.

Different approaches either to reduce or to compensate for the two first sources of error have been investigated in the past. Simultaneous or sequential bidirectional excitation schemes have been utilized to reduce some of the losses caused by laser extinction [1, 2]. Furthermore, by taking advantage of the a priori decay of intensity, iterative computer algorithms have also been employed to compensate for laser extinction [3, 4]. Accounting for signal attenuation is more complicated as it may require three-dimensional measurements, as discussed in [5]. Sick *et al.* experimented in [1] a way to estimate the local error caused by signal attenuation by measuring the transmission between the laser sheet and the camera. Finally, the correction of both laser extinction and signal attenuation was first demonstrated by Brown *et al.* [6], based on the use of a single beam. However, in spite of efforts to improve the accuracy of the local signal and even though multiple scattering has been clearly defined as the major source of errors [7, 8], no satisfying experimental solutions has been offered to account for multiple scattering issues on a planar imaging configuration until the first utilization of *Structured Laser Illumination Planar Imaging* (*SLIPI*) [9, 10].

Based on the *SLIPI* technique we demonstrate, for the first time, the possibility of extracting the local extinction coefficient within the three dimensions of an optically dense and inhomogeneous cloud of polydisperse droplets. The extinction coefficient μ_e is one of the most important optical property of a scattering and/or absorbing medium. It describes the exponential power at which a beam of light is attenuated along its incident direction as it propagates along a distance l. Assuming a homogeneous medium with constant extinction coefficient the Beer-Lambert relation can be written as: $I_f = I_i \cdot e^{-\mu_e l}$ where I_i and I_f are, respectively, the initial and final

*Corresponding author: edouard.berrocal@forbrf.lth.se

light intensity along the same direction of propagation. Note that in the optical characterization of spray systems, *extinction* is often referred in the literature to as *obscuration*. However, in the field of *light scattering by particles* the term *extinction* is widely established and mostly used [11]. From this aspect, the word *obscuration* will be avoided in the text in order to keep consistency and clarity. By definition, the extinction coefficient is defined as: $\mu_e = N \cdot [\sigma_s + \sigma_a]$ where N is the number density of droplets and σ_s and σ_a are the respective scattering and absorption cross-sections. In the case of polydisperse scattering particles, the average extinction coefficient $\overline{\mu_e}$ of an homogeneous volume is calculated as:

$$\overline{\mu_e} = N \cdot [\overline{\sigma_s} + \overline{\sigma_a}] = N \cdot \frac{\int_{D=0}^{\infty} n(D) \cdot [\sigma_s(D) + \sigma_a(D)] \cdot dD}{\int_{D=0}^{\infty} n(D) \cdot dD} \tag{1}$$

where $n(D)$ is the number of particle of diameter D. In this article a novel approach is described to extract two dimensional images of $\overline{\mu_e}$ at various depths through an aerated water spray. In order to assume that a cloud of individual droplets is probed - without the presence of a liquid core or of large irregular liquid bodies - the measurement was performed at 2.3 cm down from the nozzle tip. In this region, a minimum light transmission of only in the order of 5% transmission was measured at λ = 532 nm, corresponding to an optical depth of OD = 3.0. The type of measurement described here provides valuable quantitative information which is not accessible with conventional planar imaging owing to the multiple light scattering by droplets and interfaces.

1) Multiple light scattering intensity suppression using *SLIPI*

SLIPI is a recent laser imaging technique which has demonstrated, both experimentally [9, 10, 12] and by simulation [13], great capabilities for multiple scattering suppression in planar imaging of sprays, strongly improving visualization. The fundamental principle of the technique (originating from *structured illumination* [14]) is to use a laser sheet which is spatially modulated in intensity instead of a homogeneous laser sheet. This modulation which has a sinusoidal pattern acts as a “finger print" allowing the singly scattered photons to be recognized, as they will scatter accordingly. In contrast, photons which, after a first scattering event, deviate from their trajectory will appear as a position-dependent intensity noise on the recorded image and will not follow the modulation pattern. These photons are the multiply scattered ones. To extract the single scattering from the multiple scattering intensity, the method consists in extracting the amplitude of the modulated component in the recorded images. However, by using a single modulated illumination, parts of the probed sample are not illuminated (see Fig.1). This is compensated for by shifting the line-pattern vertically, inducing a shift on the position of the single scattering events, while the contribution from multiply scattered light remains mostly unaffected. When vertically shifting the modulation $(n-1)$ times, n images are recorded with an angular shift of $\Delta(\Phi) = 2\pi/n$ between each image. Finally, the resulting $SLIPI$, as well as the conventional image, is constructed from n modulated image according to:

$$SLIPI = \frac{\sqrt{2}}{n} \left(\sum_{j=1}^{n-1} \sum_{k=j+1}^{n} (I_j - I_k)^2 \right)^{1/2} \qquad Conv. = \frac{1}{n} \sum_{j=1}^{n} I_j \tag{2}$$

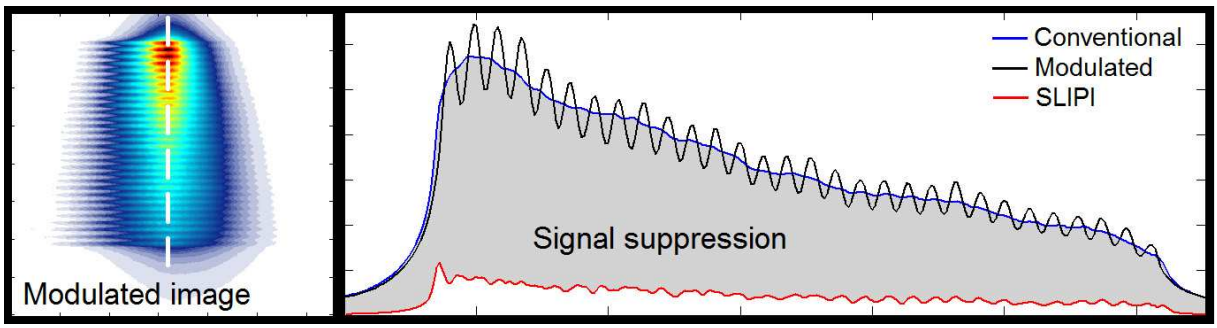

Figure 1. *Left side:* Example of a single planar image using a modulated laser sheet crossing the aerated spray. *Right side:* The black solid line shows the intensity modulation along the vertical central axis (white dashed line). Based on $n = 9$ images and Eq. 2, the *SLIPI* and the *Conv.* signals are extracted along the vertical central axis. The contribution of the unwanted light intensity introduced by multiple scattering is represented by the grey area.

In Eq. 2, I_j and I_k are intensity values and the subscript j and k denotes the different image recordings. In this equation, the pair-wise subtraction $(I_j - I_k)$ removes similar features (introduce by the indirectly scattered light) while unique features (from the directly scattered light) are kept. When averaging the n images the conventional image $Conv.$ is extracted. This image is, in theory, equal to the one acquired by using a homogeneous laser sheet, thus allowing the two techniques to be easily compared. Note that the construction of a *SLIPI* image requires a minimum of three vertically shifted images, which is the approach used in previous studies [9, 10, 12, 13]. Increasing the number of images leads to a more narrow line displacement. Although time consuming, this improves the effectiveness of the suppression, especially for scattering media containing strong vertical variations. Another issue that may be improved when using smaller line displacement, concerns the presence of residual line structures on the *SLIPI* images. These artifacts arise when the contribution of directly scattered light differs between the intensity modulated images and becomes more visible when the single scattering contribution is reduced. Spatial changes in the laser profile may also give rise to such unwanted effects. Methods to reduce these residuals are described in [15] but may not always be sufficient. By using a larger number n of images, the presence of these artifacts can be statistically reduced. For this reason, nine modulated images, instead of three, have been used in this article to reconstruct both the *SLIPI* image at successive depth within the spray.

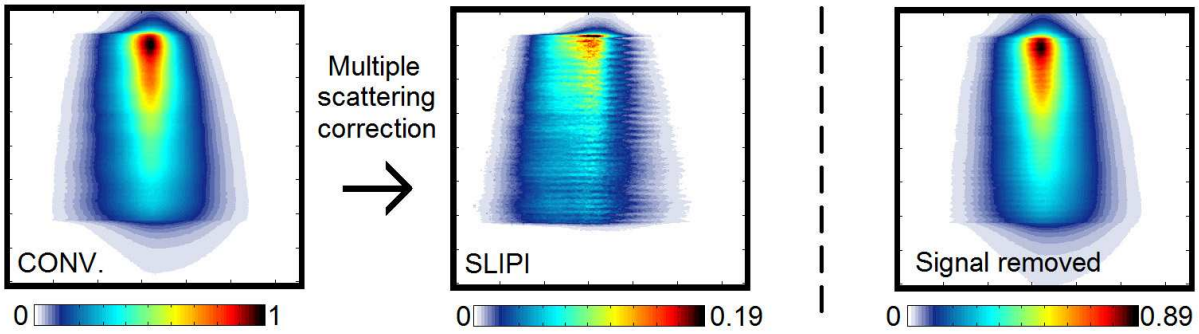

Figure 2. *Left side:* Example of the conventional and *SLIPI* images built up from 9 modulated images where the spatial phase Φ is shifted 8 times by $\Delta(\Phi) = 2\pi/9$. *Right side:* The maximum light intensity removed from the conventional image almost reaches 90% in the region closest to the nozzle tip. The light intensity (photon counts) has been normalized with the maximum value of the conventional image.

2) Experimental set-up

The laser source consisted of a frequency doubled Nd:YAG laser, λ = 532 nm, operating at 10 Hz repetition rate. A small portion of the central gaussian beam was selected and spatially filtered to create an initial near top-hat intensity distribution. The line structures were formed using a transmission Ronchi grating and were shifted vertically by tilting a 1 mm glass plate. The slightly diverging laser sheet was created by combining two oppositely orientated positive cylindrical lenses and was 3.3 cm high in the measurement region. The resulting spatial period of the modulation was 1.15 mm (distance between the lines). The laser sheet was vertically shifted 8 times with a displacement of 128 μm between images to produce the nine required modulated images. At each of the nine positions an average over 500 accumulation was recorded by a 14-bit Electron Multiplying CCD camera (iXon-897, 512 X 512 pixels). To keep the contribution of multiple scattering as low as possible the full angle of the collection optics was fixed as small as possible such that $\theta_{co} = 1.35^\circ$. This was obtained by choosing a f-number $F\#$ = 8 on a Nikkon 200 mm focal length objective. The imaged area was situated at 2.3 cm below the nozzle tip and included the spray itself and a cuvette containing a solution of Rhodamine 6G which was located next to the spray. This dye cell was illuminated by the laser sheet after crossing the spray and provides a measurement of the light transmission. Furthermore, a portion of the incident beam was extracted and guided around the spray to the dye cell in order to monitor the pulse-to-pulse intensity fluctuation. To obtain the value of the extinction coefficient in three dimensions, *SLIPI* images of the spray and the dye cuvette were recorded for 30 successive planes, where the nozzle was translated perpendicularly to the laser sheet with a step of 500 μm between each image. This scanning process was performed from the edge to the centre of the spray (corresponding to a distance of 1.5 cm), resulting in an increase of the signal attenuation at each translation step.

In the present experiment the nozzle used was a Delavan AL-45 of tip diameter d = 3 mm, producing a narrow angle spray pattern with a nominal angle of $15^\circ - 20^\circ$ in ambient air. This air assisted nozzle, is an internal mixing nozzle, where a change in air or liquid injection pressure results in a change of flow or atomization. Increasing air

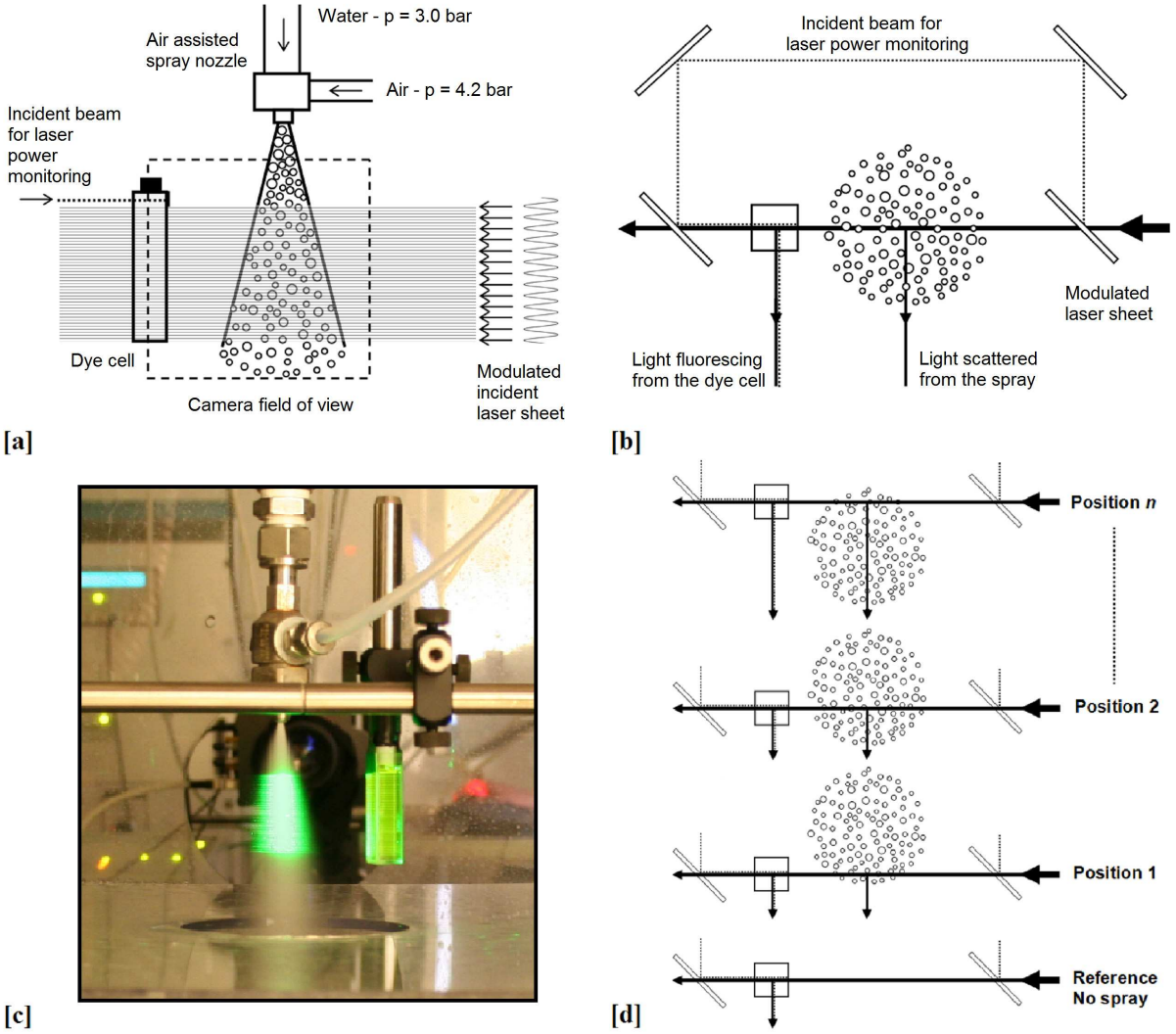

Figure 3. Description of the experimental set-up: [a] Side view - An intensity modulated laser sheet crossing an aerated water spray and a dye cell containing a solution of Rhodamine 6G is imaged at 90° with an EM-CCD camera. [b] Top view - A portion of the the incident laser beam is extracted and counter propagates through the dye cell in order to monitor the laser power fluctuation. [c] Picture of the aerated water spray which is imaged at 2.3 cm from the nozzle tip. The spray is running at 3.0 bar water pressure and 4.2 bar air pressure resulting to a 21 l/hour liquid flow and 175 l/min air flow. [d] The spray is scanned by recording images with a distance of 500 μm between each successive position. Scanning half of the spray requires a number of 30 *SLIPI* images, covering a distance of 1.5 cm. Each *SLIPI* image is constructed using 9 shifted modulated images. Each of these modulated images are averaged from 500 single-shots.

pressure decreases flow and increases atomization while increasing liquid pressure increases flow and decreases atomization. The investigated spray was running in steady state at 3 bar water pressure and 4.2 bar air pressure delivering, in ambient air, a liquid flow rate of 21 l/hour and an air flow rate of 175 l/min. Due to the internal mixing, breakups occur already at the nozzle tip exit producing a dense elongated cloud of fine droplets of $\sim$ 15 μm nominal diameter (droplet size provided by the manufacturer).

3) Correction for signal attenuation and laser extinction

In this section, the procedure to extract the extinction coefficient distribution within each of the 30 *SLIPI* planes is described. As explained previously, a single *SLIPI* image represents the light intensity which is close to the pure single light scattering intensity (as demonstrated in [13]). However, these images are still affected by the attenuation of the emitted signal between the laser sheet and the camera and by the extinction of the laser sheet

as it propagates through the spray. As a result, the *SLIPI* images must be adequately processed in order to obtain valuable quantitative information regarding the optical properties of the spray. The mathematical procedure to correct for signal attenuation and laser extinction is based on the Beer-Lambert law and is described as follows: The collected data are two dimensional *SLIPI* images with pixels covering a sample area of $(\delta x, \delta y)$ (corresponding to 166 X 166 μm). Images separated by a distance δz (corresponding to 500 μm) in the sample are stacked on top of each other to form a three dimensional matrix as depicted in Fig. 4. The center of the voxels named (k, l, m) are positioned at: $\left(\left(k-\frac{1}{2}\right)\delta x, \left(l-\frac{1}{2}\right)\delta y, \left(m-\frac{1}{2}\right)\delta z\right)$ where k, l and m are integers ranging from one to the number of pixels in the X and Y direction, and to the number of images in the Z direction. The recorded signal *SLIPI*(k, l, m), corresponds to the voxel (k, l, m) in the sample can be expressed as:

$$SLIPI(k,l,m) = P(k,l,m)K(k,l,m)\exp\left(-\sum_{m'=0}^{m-1}\overline{\mu_e}(k,l,m')\delta z\right), \tag{3}$$

where $P(k, l, m)$ represents the radiant power of the light scattered from voxel (k, l, m) and $K(k, l, m)$ contains the solid angle of detection and the collection efficiency of the camera. The exponential term, with the extinction coefficient $\overline{\mu_e}$, represents the signal attenuation as the light propagates from voxel (k, l, m) through the sample to the camera. Here the camera is positioned at $m = -\infty$ with a small enough detection angle for the light only to travel along Z at its original position in the X and Y direction. From Eq. 3 the radiant power P can be expressed as:

$$P(k,l,m) = \frac{SLIPI(k,l,m)}{K(k,l,m)\exp\left(-\sum_{m'=0}^{m-1}\overline{\mu_e}(k,l,m')\delta z\right)} \tag{4}$$

The sum of the radiant power scattered from each voxel along a row of voxels in the direction of the laser sheet is equal to the difference between the incoming and exiting power of the laser light such that,

$$\sum_{k=1}^{k_{max}} P(k,l,m) = \delta y \delta z (I(0,l,m) - I(k_{max},l,m)) \tag{5}$$

Entering Eq. 4 into Eq. 5 yields

$$\sum_{k=1}^{k_{max}} \frac{SLIPI(k,l,m)}{K(k,l,m)\exp\left(-\sum_{m'=0}^{m-1}\overline{\mu_e}(k,l,m')\delta z\right)} = \delta y \delta z (I(0,l,m) - I(k_{max},l,m)) \tag{6}$$

If the collection efficiency K is assumed to be independent on the position of the scattering event along X, then it can be moved outside the summation and expressed as the ratio between the integrated signal over the laser path compensated for the signal attenuation and the power of the scattered light over the same path.

$$K(k,l,m) = \sum_{k=1}^{k_{max}} \frac{SLIPI(k,l,m)}{\exp\left(-\sum_{m'=0}^{m-1}\overline{\mu_e}(k,l,m')\delta z\right)} \left(\delta y \delta z (I(0,l,m) - I(k_{max},l,m))\right)^{-1} \tag{7}$$

By replacing the collection efficiency K in Eq.4 with the expression in Eq. 7 one get

$$P(k,l,m) = \frac{SLIPI(k,l,m)\delta y \delta z ((I(0,l,m) - I(k_{max},l,m)))}{\exp\left(-\sum_{m'=0}^{m-1}\overline{\mu_e}(k,l,m')\delta z\right)\sum_{k=1}^{k_{max}} \frac{SLIPI(k,l,m)}{\exp\left(-\sum_{m'=0}^{m-1}\overline{\mu_e}(k,l,m')\delta z\right)}} \tag{8}$$

The only unknown parameters in Eq. 8 is the extinction coefficient. However, if the plane closest to the camera is located at the edge of the sample, the attenuation of the signal generated within this plane can be neglected. Hence for $m = 1$ the scattered signal $P(k, l, 1)$ can be calculated from the *SLIPI* and the transmission measurement only.

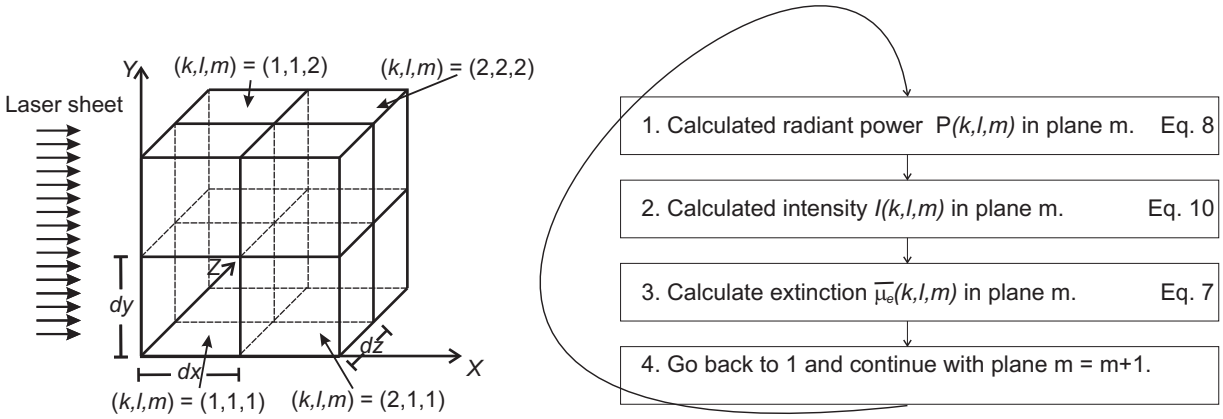

Figure 4. *Left side:* Illustration of the 3D coordinate system (X, Y, Z) which is composed of individual homogeneous voxels identified by their location (k, l, m). *Right side:* Description of the procedure to correct the *SLIPI* images from signal attenuation and laser extinction in order to extract the extinction coefficient.

The next step is to calculate the position dependent laser intensity and extinction coefficients in the voxels where the scattered radiant power have been calculated. This can be done by relating the intensity of a voxel to the intensity in the previous voxel using Beer Lamberts law

$$I(k+1,l,m) = I(k,l,m)\exp\left(-\overline{\mu_e}(k,l,m)\delta x\right) \tag{9}$$

Since the intensity in the voxel can also be expressed as the intensity in the previous voxel minus the scattered intensity,

$$I(k+1,l,m) = I(k,l,m) - \frac{P(k,l,m)}{\delta y \delta z} \tag{10}$$

insertion of Eq. 10 into Eq. 9 gives an expression of the extinction coefficient:

$$\overline{\mu_e}(k,l,m) = -\ln\left(\frac{I(k,l,m) - \frac{P(k,l,m)}{\delta y \delta z}}{I(k,l,m)}\right)\frac{1}{\delta x} \tag{11}$$

From Eq. 10 the intensity can be calculated whereafter Eq. 11 can be used to calculate $\overline{\mu_e}$. In the $m = 2$ plane, Eq. 8 is used to calculate the position dependent radiant power. The attenuation of the signal is now nonzero. However, since the extinction coefficients have already been calculated for the plane $m = 1$ the exponentials in the denomination of Eq.8 will compensate for this. The procedure is repeated until the radiant power of the scattered light, the intensity and the extinction coefficients are calculated for every voxel in the entire matrix. An overview of the algorithm is provided in Fig. 4 while an example of processed images is given in Fig. 5.

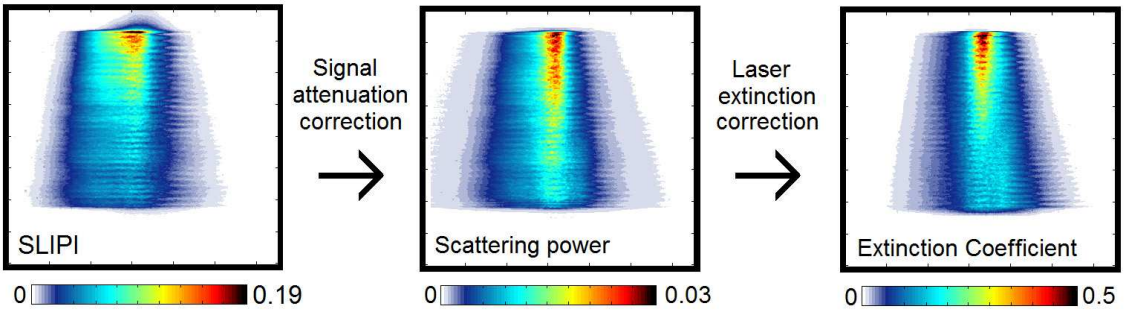

Figure 5. Example of image processing from the *SLIPI* image (light intensity) to an image showing the spatial distribution of the extinction coefficient $\overline{\mu_e}$ (in mm^{-1}). These images correspond to the central axis of the spray.

4) Results

By operating the algorithm described in the previous section to the successive *SLIPI* images, the local averaged extinction coefficient $\overline{\mu_e}$ is extracted over the spray. Figure 6 shows these results for 8 planes, from the centre toward the edge of the spray, with 1 mm step between images. It can be seen that the maximum $\overline{\mu_e}$ equals 0.5 mm^{-1} and is, as expected, located in the region the closest to the nozzle tip. On the opposite, the minimum $\overline{\mu_e}$ equals $\sim$0.01 mm^{-1} and is located on the spray edge. In addition to these data, the optical depth OD is shown in Fig. 7, for both the path between the laser sheet and the camera and along the laser sheet. Note that OD corresponds to the integration of $\overline{\mu_e}$ along the path traveled by the photons for a given direction.

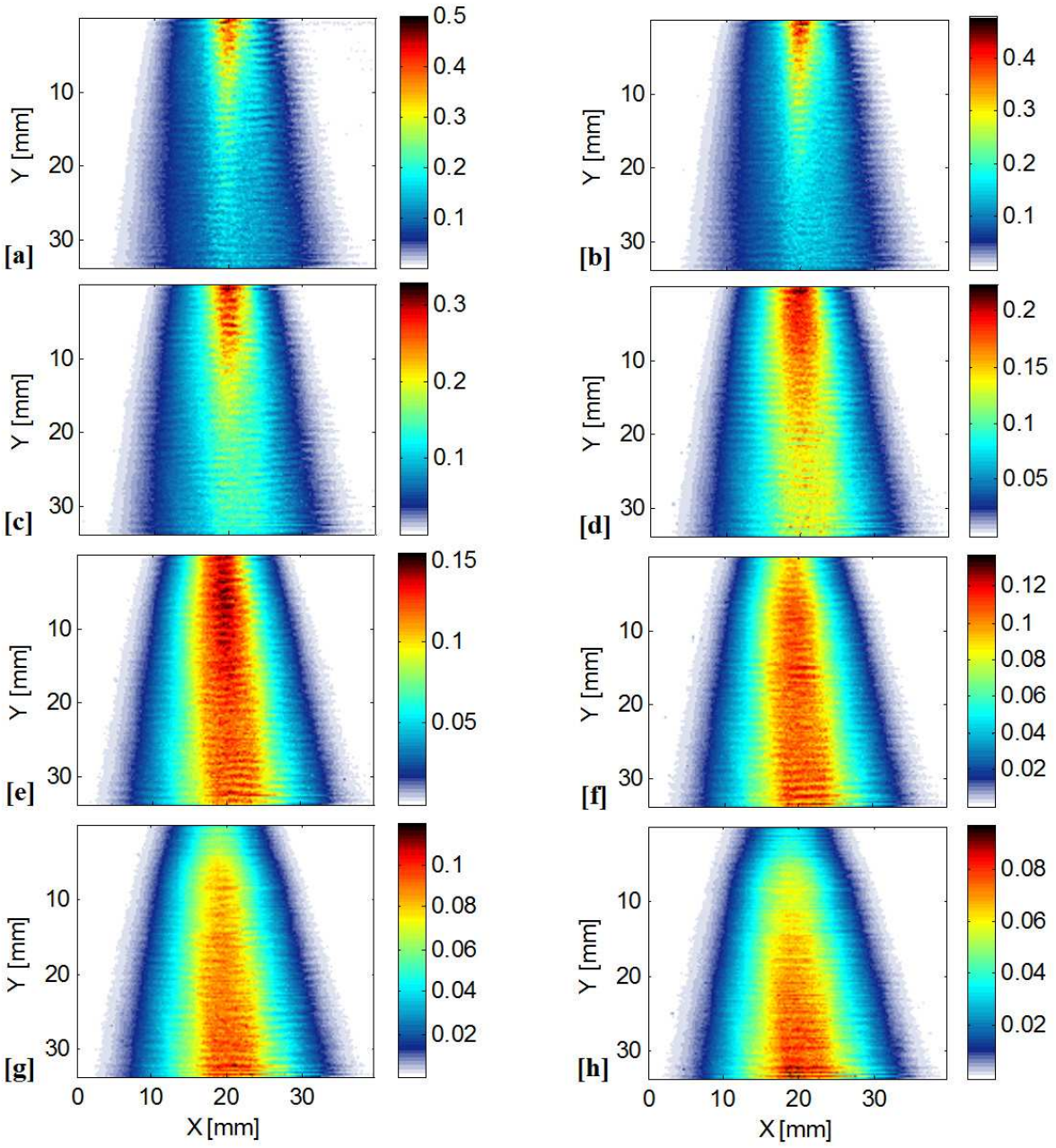

Figure 6. Two-dimensional quantitative distribution of the extinction coefficient $\overline{\mu_e}$ (in mm^{-1}) at different depths through the spray. The nozzle tip is located 23 mm above the images. [a] corresponds to the central axis of the spray, [b] is 1 mm off-axis, [c] is 2 mm off-axis, [d] is 3 mm off-axis, [e] is 4 mm off-axis, [f] is 5 mm off-axis, [g] is 6 mm off-axis and [h] is 7 mm off-axis from the centre of the spray. This succession of images clearly shows the reduction of the extinction coefficient as the plane of consideration is getting closer to the spray edge.

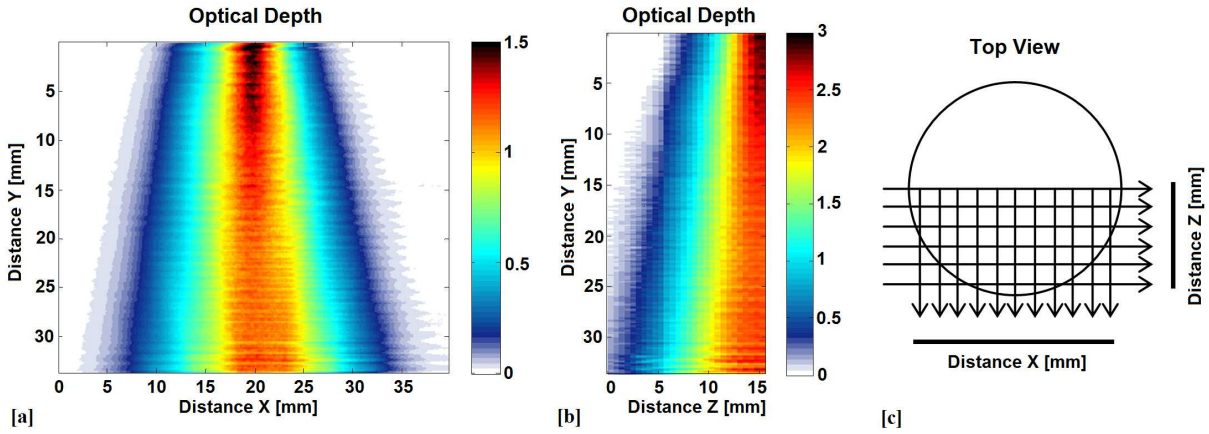

Figure 7. Two-dimensional quantitative distribution of the optical depth between the central spray axis and the camera in [a] and along the laser path in [b]. A schematic is shown in [c] for a better understanding of the measured quantities. In [a] OD is calculated by the sum of $\overline{\mu_e} \cdot \delta z$ over the 30 plane positions of the laser sheet within the spray (shown in Fig. 6). The OD shown in [b] is extracted from the transmission measurement, based on the *SLIPI* images (multiple scattering suppression) of the dye cell (see Fig. 3). This image shows the OD results of the 30 positions of the laser sheet in the spray, explaining the reduced image resolution (each pixel representing an area of 500 X 166 μm). It is observed from these results that the maximum OD in [b] is twice as large as the maximum OD in [a]. At the same time, the distance in [b] is twice as large as in [a], demonstrating a good symmetry of the spray system.

Conclusion

We have demonstrated in this article the possibility of extracting the local averaged extinction coefficient within the three dimensions of an optically dense aerated water spray. This was performed by first removing the multiple light scattering intensity in both planar laser Mie imaging and transmission measurements. The suppression was achieved by means of a recently developed technique called *SLIPI*. By using this technique and progressively sampling different depths, a three dimensional representation of the spray was acquired. A correction procedure, based on the Beer-Lambert law, to account for both signal attenuation and laser extinction was then implemented on these results. It is demonstrated how this approach provides quantitative information in three dimensions and the extracted quantity - the extinction coefficient - is of fundamental importance as it represents the true nature of the probed sample, in opposition to signal intensity which is hampered by both extinction and attenuation. In addition, this complete characterization was obtained using affordable and standard laser and camera equipment.

Acknowledgement

Finally, the authors wish to show their appreciation to the Linné Center within the Lund Laser Center (LLC) as well as CECOST through SSF and STEM for financial support. The authors would like to also acknowledge the support of the European Research Council (ERC).

References

[1] V. Sick and B. Stojkovic, Appl. Opt. 40 (2001) 2435-2442.
[2] M. Versluis, N. Georgiev, L. Martinsson, M. Alden, S. Kroll, Appl. Phys. B 65 (1997) 411-417.
[3] H. M. Hertz and M. Aldén, Appl. Phys. B 42 (1987) 97-102.
[4] R. Abu-Gharbieh, J. L. Persson, M. Forsth, A. Rosen, A. Karlstrom, and T. Gustavsson, Appl. Opt. 39 (2000), 1260-1267.
[5] K. Inagaki, S. Miura, K. Nakakita, and S. Watanabe, "Quantitative Soot Concentration Measurement with the Correction of Attenuated Signal Intensity Using Laser-Induced Incandescence," *Proceeding of the 4th International Symposium COMODIA*, (1998).
[6] C. T. Brown, V. G. McDonell, and D. G. Talley, Accounting for laser extinction, signal attenuation, and secondary emission while performing optical patternation in a single plane, Proceeding of the 15th ILASS-America, Madison, USA, 2002.
[7] M.C. Jermy and D.A. Greenhalgh, Appl. Phys. B 71 (2000) 703-710

[8] E. Berrocal, *Multiple scattering of light in optical diagnostics of dense sprays and other complex turbid media*, PhD Thesis, Cranfield University, Bedfordshire, England, 2006.
[9] E. Kristensson, E. Berrocal, M. Richter, S.-G. Pettersson, and M. Aldén, Opt. Lett. 33 (2008) 2752-2754.
[10] E. Berrocal, E. Kristensson, M. Richter, M. Linne, and Marcus Aldén, Opt. Express, 16 (2008) 17870-17881.
[11] C. F. Bohren and D. R. Huffman, *Absorption and Scattering of Light by Small Particles*, Wiley-VCH, 1983.
[12] E. Kristensson, E. Berrocal, M. Richter and M. Linne, Ultra-fast Structured Laser Illumination Planar Imaging (SLIPI) for single-shot imaging of dense sprays, Proceeding of the 11th ICLASS, Vail, USA, 2009.
[13] E. Berrocal, E. Kristensson, D. Sedarsky, M. Aldén, and M. Linne, Analysis of the SLIPI technique for multiple scattering suppression in planar imaging of fuel sprays, Proceeding of the 11th ICLASS, Vail, USA, 2009.
[14] M. A. A. Neil, R. Juskatitis, and T. Wilson, Opt. Lett. 22 (1997) 1905-1907.
[15] L. H. Schaefer, D. Schuster, and J. Schaffer, J. Microsc. 22 (2004) 165-174.